Ecography

ECOG-05181

Young, M. A., Treml, E. A., Beher, J., Fredle, M., Gorfine, H., Miller, A. D., Swearer, S. E. and Ierodiaconou, D. 2020. Using species distribution models to assess the long-term impacts of changing oceanographic conditions on abalone density in south east Australia. – Ecography doi: 10.1111/ecog.05181

Supplementary material

Appendix 1

Methods

Hydrodynamic Modelling

Hydrodynamic data quantifying the nearshore and far-field ocean currents around Victoria and the regional seascape were obtained from Water Technology for local-scale depth-averaged and high spatial-temporal resolution products. Water Technology coupled a hydrodynamic (HD) and spectral wave (SW) model using the industry standard hydrodynamic software package MIKE by DHI (Danish Hydraulics Institute) with input from the research team. The approach uses a variable resolution depth-averaged approach to quantify currents along the Victorian coastline, including tides, winds, bottom rugosity, and regional forcing. Water level boundaries were applied to simulate tides. No wave boundaries were applied to the model as the domain extends past the extents of the Victorian coast and south to a latitude of -45 degrees, thus allowing swell to develop far offshore as well as local sea near the coast. Wind and pressure data were provided through the NCEP-DOE Reanalysis 2 model run by the Earth System Research Laboratory (ESRL) at the National Oceanic and Atmospheric Administration (NOAA) in the USA. Astronomical tidal conditions were applied to the model boundaries from a global model developed by DHI. The source data for tidal prediction is based on 10 tidal constituents with a grid resolution of 7.5 minutes. The tidal boundaries applied to the model have a spatial variation step of 13 km and a time step of 1 hour. The model domain consists of a flexible mesh incorporating triangular and quadrilateral elements of various sizes (Figure A1, Figure A2). This approach allows for detail in land boundaries and increased resolution in areas of particular interest or important variations in bathymetry, while also reducing the resolution and number of elements in the ocean. The elements range in size from around 700 km^2 offshore to less than 1 km^2 near the

coast. The model extends from 45.00 to 37.50 degrees south, and 138.75 to 125.25 degrees east. This includes the whole Victorian and Tasmanian coasts and into South Australia and New South Wales. Extending the model domain allows swell wave development within the model negating the need for wave boundaries for our study area of interest.

Spectral wave conditions were developed from the input wind conditions. The spectrum was divided into 25 frequencies logarithmically distributed with a factor of 1.1 from 0.05 Hz. The directional spectra was divided into 16 bins. The time step for spectral wave calculations was limited to between 0.01 and 720 seconds. Temperature and salinity were not included in the model as independent variables, rather they are set at constant 10°C and 32 PSU. A constant Manning's bed resistance of 0.02 $m^{1/3}s^{-1}$ was applied across the model domain. Coriolis forcing was varied across the domain as it extends over 2.50 degrees in latitude. A Smagorinsky formulation was used for the horizontal eddy viscosity with a constant of 0.28.

Downscaled coupled wave and hydrodynamic models were provided in DHI-MIKE format for 1990 to 2015 in annual files describing ocean currents at a 5 minute time-step with a spatial resolution of ~500m at the shoreline to ~10km in Bass Strait, and to ~30km in the open ocean. Each simulation was started from still conditions with water levels and wave conditions then developed from the boundary conditions applied. Model results were output for the whole computational domain with a temporal resolution of 1 hr. Results were divided into hydrodynamic and spectral wave outputs resulting in two result files for each year of simulation. The raw results have data for each computational element across the domain, these outputs have been further processed prior to delivery.

The output parameters included were:

- Surface elevation
- Total water depth
- Depth averaged current vectors
- Significant wave height

- Wave period T02
- Mean wave direction
- Wave power

Monthly wave statistics have been calculated for the modelled period and interpolated to a regular grid along the Victorian coast. Parameters derived include:

- Current speed (max, avg)
- Significant wave height (max, avg)
- Wave period for max significant wave height.
- Orbital velocity (max, avg)
- Wave power (max, avg)

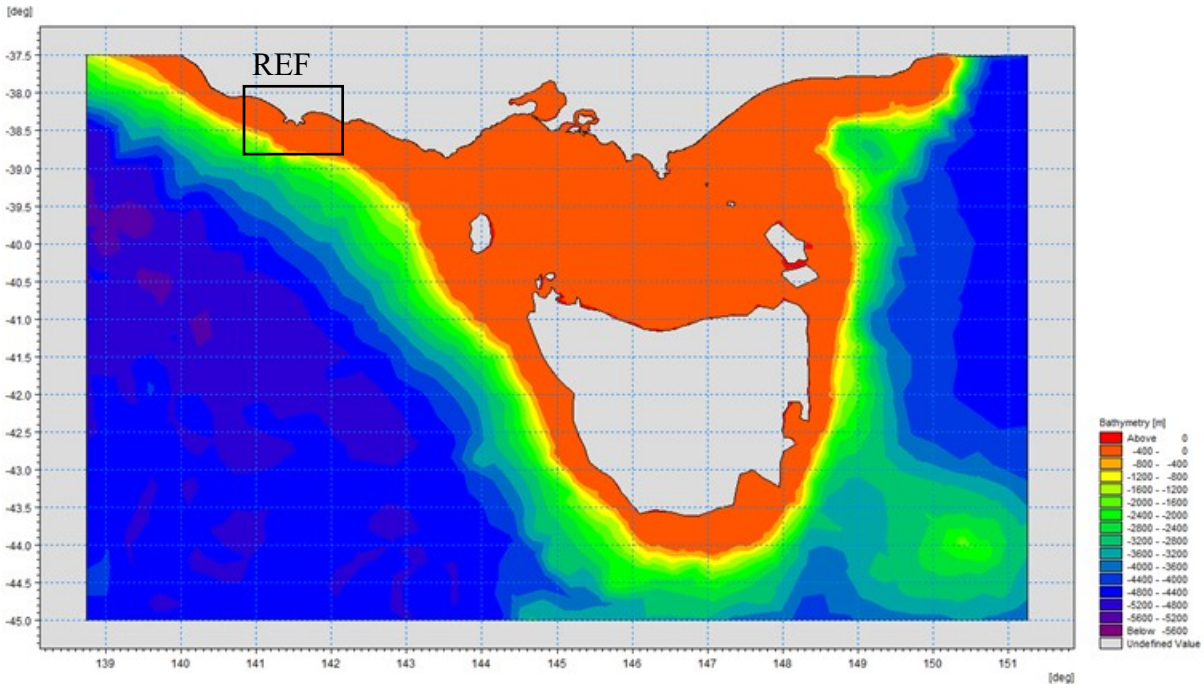

Figure A1: Model domain shown in Danish Hydraulics Institute software.

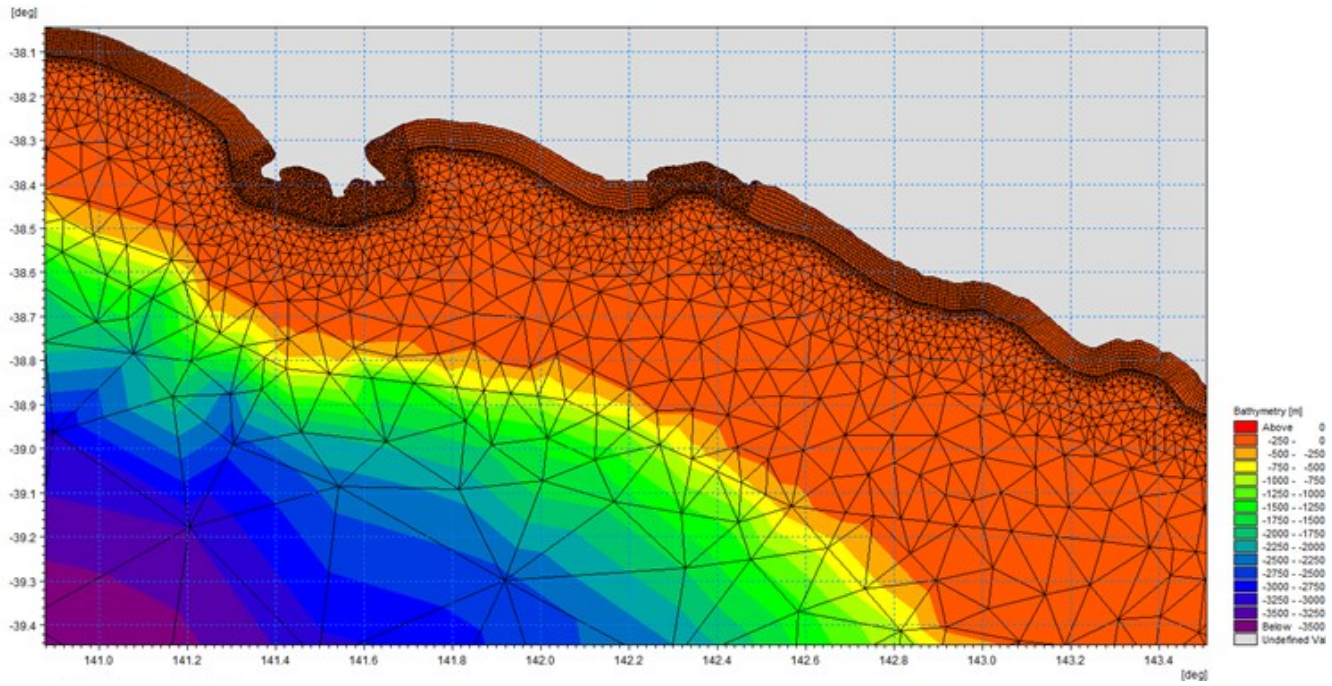

Figure A2: Mesh elements in the zoomed-in section from Figure A1 for the hydrodynamic model.

Table A1: Summaries and definitions of the explanatory variables investigated in the Boosted Regression Tree models for abalone productivity.

Variable Type	Variable	Variable Code	Description	Variable Source	Used in Final BRT (Y/N)?
Time	Quota Year	QuotaYear	The quota year associated with each biomass value was used as a factor in the model.	Fisheries Victoria abalone abundance surveys	N
	Grouped Quota Year	QuotaYearG	Clustered groups of years with similar biomass values Clusters were derived using the TSclust package in R (Montero and Vilar, 2014) and 7 time frames were defined.	Fisheries Victoria abalone abundance surveys	N
AVG	Spatial and temporal location of AVG outbreak	AVG_Inf	For each year, the biomass data were categorised into four classes associated with the AVG outbreak: "0" for years pre-outbreak and those areas not affected by the virus, "3" for the spatial extent of the AVG outbreak from 2006-2008 (during outbreak), "2" for the spatial extent of the AVG outbreak in the 2 years following the outbreak, and "1" for the spatial extent of the AVG outbreak 3-5 years after the outbreak.	Spatial categorical maps were developed from virus outbreak observations (Gorfine et al. 2008).	Y

Hydro-Dynamics	Average Current Speed	ACS_an ACS_s ACS_w	Annual, summer, and winter average current speeds were calculated for each year from 1990 to 2015. The original dataset was provided at 500 m resolution and were then downscaled to 30 m using Empirical Bayesian Kriging.	Water Technology hydrodynamic models	N
	Average Significant Wave Height	ASWH_an ASWH_s ASWH_w	Annual, summer, and winter average significant wave heights were calculated for each year from 1990 to 2015. The original dataset was provided at 500 m resolution and were then downscaled to 30 m using Empirical Bayesian Kriging.	Water Technology hydrodynamic models	N
	Average Wave Orbital Velocity	AWOV_an AWOV_s AWOV_w	Annual, summer, and winter average wave orbital velocities were calculated for each year from 1990 to 2015. The original dataset was provided at 500 m resolution and were then downscaled to 30 m using Empirical Bayesian Kriging.	Water Technology hydrodynamic models	N
	Average Wave Power	AWP_an AWP_s AWP_w	Annual, summer, and winter average wave powers were calculated for each year from 1990 to 2015. The original dataset was provided at 500 m resolution and were then downscaled to 30 m using Empirical Bayesian Kriging.	Water Technology hydrodynamic models	N
	Current Direction	CD_an CD_s CD_w	Annual, summer, and winter average current directions were calculated for each year from 1990 to 2015. The original dataset was provided at 500 m resolution and were then downscaled to 30 m using Empirical Bayesian Kriging.	Water Technology hydrodynamic models	N
	Maximum Current Speed	MCS_an MCS_s MCS_w MCS_an	Annual, summer, and winter maximum current speeds were calculated for each year from 1990 to 2015. The original dataset was provided at 500 m resolution and were then downscaled to 30 m using Empirical Bayesian Kriging.	Water Technology hydrodynamic models	Y
	Maximum Significant Wave Height	MSWH_an MSWH_s MSWH_w	Annual, summer, and winter maximum significant wave heights were calculated for each year from 1990 to 2015. The original dataset was provided at 500 m resolution and were then downscaled to 30 m using Empirical Bayesian Kriging.	Water Technology hydrodynamic models	N
	Maximum Wave Orbital Velocity	MWOV_an MWOV_s MWOV_w	Annual, summer, and winter maximum wave orbital velocities were calculated for each year from 1990 to 2015. The original dataset	Water Technology hydrodynamic models	Y

			was provided at 500 m resolution and were then downscaled to 30 m using Empirical Bayesian Kriging.		
	Maximum Wave Power	MWP_an MWP_s MWP_w	Annual, summer, and winter maximum wave powers were calculated for each year from 1990 to 2015. The original dataset was provided at 500 m resolution and were then downscaled to 30 m using Empirical Bayesian Kriging.	Water Technology hydrodynamic models	N
	Wave Period	WP_an WP_s WP_w	Annual, summer, and winter wave periods were calculated for each year from 1990 to 2015. The original dataset was provided at 500 m resolution and were then downscaled to 30 m using Empirical Bayesian Kriging.	Water Technology hydrodynamic models	N
Seafloor Structure	Depth	depth	Water depth for each cell in the gridded data derived from the LiDAR/multibeam bathymetry data. Depth values were resampled to 30 m resolution.	Merged LiDAR/ multibeam dataset	Y
	Slope	slope	Maximum change in depth from each cell in its three-by-three neighbourhood. Calculated using the "Slope" tool in ArcGIS Spatial Analyst at 5 m resolution. Slope values were then resampled to 30 m resolution.	Merged LiDAR/ multibeam dataset	N
	Vector Ruggedness Measure (VRM)	vrm	A measure of surface roughness taking into account the aspect and slope in a three-by-three neighbourhood. VRM was calculated using the "VRM" tool in the Benthic Terrain Modeler (BTM; Wright et al. 2012) at 5 m resolution. VRM values were then resampled to 30 m resolution.	Merged LiDAR/ multibeam dataset	Y
	Bathymetric Position Index (BPI)	BPI50 BPI100 BPI50 BPI250 BPI500	A measure of a cell's depth relative to its surrounding cells at a defined scale (50 m, 100 m, 250 m, and 500 m scales were computed). VRM was calculated using the "Broad Scale BPI" tool in the Benthic Terrain Modeler (BTM; Wright et al. 2012) at 5 m resolution. BPI values were then resampled to 30 m resolution.	Merged LiDAR/ multibeam dataset	Y
	Substrate	substrate	Seafloor substrate type ("reef", "mixed", "sediment") derived from bathymetry and backscatter and then manually edited to remove artefacts.We used a decision tree classification (outlined in	Merged LiDAR/ multibeam dataset	N

			Ierodiaconou et al. 2011 and Zavalas et al. 2014) to distinguish between rock and sediment. Then, manually edited the resulting classification to remove any areas of misclassification based on thresholds of VRM.		
	Reef Area	reef_area	Area of each reef from the "reef" class in the substrate raster.	Merged LiDAR/ multibeam dataset	Y
Connec-tivity	In Degree	d_indeg_an	The total number of 'significant' connections coming into a destination site.	Output from biophysical modelling	Y
	Local Retention	d_lr_an	Proportion of larvae released that settle back to the source site.	Output from biophysical modelling	N
	Self Recruitment	d_sr_an	The relative proportion of settlers at each destination site that originated from that focal site.	Output from biophysical modelling	Y
	Total Inflow	d_totin_an	Total relative inflow from all sites including local retention.	Output from biophysical modelling	N
Catch Data	Zone Catch Data	WCE_catch WCE_CPUE	The total catch and CPUE from each of the commercial abalone fishing zones (Western, Central, Eastern) from 1995 to 2015 were weighted by the availability of reef habitat in each zone.	Victorian Fisheries Authority Catch Data	N
	Sub-Zone Catch Data	SZ_catch SZ_CPUE	The total catch and CPUE from each of the commercial abalone fishing subzones from 1995 to 2015 were weighted by the availability of reef habitat in each subzone.	Victorian Fisheries Authority Catch Data	N

Table A2: Category names assigned during the Emerging Hot Spot Analysis and definition of each of the patterns observed within those categories. This table is recreated from the ArcMap Emerging Hot Spot Analysis help documentation (ESRI 2011).

Pattern Name	Definition
No Pattern Detected	Does not fall into any of the hot or cold spot patterns defined below
New Hot Spot	A location that is a statistically significant hot spot for the final time step and has never been a statistically significant hot spot before.
Consecutive Hot Spot	A location with a single uninterrupted run of statistically significant hot spot bins in the final time-step intervals. The location has never been a statistically significant hot spot prior to the final hot spot run and less than ninety percent of all bins are statistically significant hot spots.

Intensifying Hot Spot	A location that has been a statistically significant hot spot for ninety percent of the time-step intervals, including the final time step. In addition, the intensity of clustering of high counts in each time step is increasing overall and that increase is statistically significant.
Persistent Hot Spot	A location that has been a statistically significant hot spot for ninety percent of the time-step intervals with no discernible trend indicating an increase or decrease in the intensity of clustering over time.
Diminishing Hot Spot	A location that has been a statistically significant hot spot for ninety percent of the time-step intervals, including the final time step. In addition, the intensity of clustering in each time step is decreasing overall and that decrease is statistically significant.
Sporadic Hot Spot	A location that is an on-again then off-again hot spot. Less than ninety percent of the time-step intervals have been statistically significant hot spots and none of the time-step intervals have been statistically significant cold spots.
Oscillating Hot Spot	A statistically significant hot spot for the final time-step interval that has a history of also being a statistically significant cold spot during a prior time step. Less than ninety percent of the time-step intervals have been statistically significant hot spots.
Historical Hot Spot	The most recent time period is not hot, but at least ninety percent of the time-step intervals have been statistically significant hot spots.
New Cold Spot	A location that is a statistically significant cold spot for the final time step and has never been a statistically significant cold spot before.
Consecutive Cold Spot	A location with a single uninterrupted run of statistically significant cold spot bins in the final time-step intervals. The location has never been a statistically significant cold spot prior to the final cold spot run and less than ninety percent of all bins are statistically significant cold spots.
Intensifying Cold Spot	A location that has been a statistically significant cold spot for ninety percent of the time-step intervals, including the final time step. In addition, the intensity of clustering of low counts in each time step is increasing overall and that increase is statistically significant.
Persistent Cold Spot	A location that has been a statistically significant cold spot for ninety percent of the time-step intervals with no discernible trend, indicating an increase or decrease in the intensity of clustering of counts over time.
Diminishing Cold Spot	A location that has been a statistically significant cold spot for ninety percent of the time-step intervals, including the final time step. In addition, the intensity of clustering of low counts in each time step is decreasing overall and that decrease is statistically significant.
Sporadic Cold Spot	A location that is an on-again then off-again cold spot. Less than ninety percent of the time-step intervals have been statistically significant cold spots and none of the time-step intervals have been statistically significant hot spots.
Oscillating Cold Spot	A statistically significant cold spot for the final time-step interval that has a history of also being a statistically significant hot spot during a prior time step. Less than ninety percent of the time-step intervals have been statistically significant cold spots.
Historical Cold Spot	The most recent time period is not cold, but at least ninety percent of the time-step intervals have been statistically significant cold spots.

Biophysical Modelling

We developed a new parametrisation of our biophysical dispersal model (Treml, et al. 2012, Treml, et al. 2015) to quantify the population connectivity patterns for the *H. rubra* fishery occurring across Victoria's seascape. This modelling approach incorporates species-specific habitat, oceanographic, and biological data to effectively estimate the probability for larvae to successfully disperse from potential source habitat sites to all destination habitat patches. Dispersal simulations were carried out by releasing a cloud of larvae into the model seascape at all individual habitat patches and allowing larvae to be transported downstream with currents. Ocean current velocities, turbulent diffusion, and larval behaviour move the larvae through the seascape at each modelled time-step. Larval competency, behaviour, and mortality determine when and what proportion of larvae settle in habitat patches at each time step. When larvae encounter habitat, the concentration of larvae settling with the habitat patch is recorded at that time-step. Dispersal simulation data were saved in the form of a 3-D dispersal matrix representing the cumulative quantity of larvae released from each source patch *i* that have settled on any destination patch *j* throughout the entire dispersal period. This matrix was used to calculate the pair-wise dispersal probability of moving from each source to destination, [P] matrix, and the migration matrix, [M], representing the likelihood that a settler to destination patch originated from each potential upstream source patch (Treml et al. 2012). Habitat and species-specific life history parameters were used for the abalone and SRL (Table A2). All connectivity analyses were derived from these two matrices, as outlined below.

Table A3: Parameters used in the biophysical modelling of larval dispersal for *Haliotis rubra*.

Parameter	Abalone Model
Model extent	Victorian coastline, including Bass Strait (Figure A3)
Model resolution	1 km
Hydrodynamic Data Used	DHI-Mike coastal model – Water Technology
Habitat Requirements	Hard substrate within 10-meter depth
Adult density	Relative to amount of habitat per patch
Daily larval mortality	5% per day
Time to reach competency and/or mobility for settlement	4.5 days +/- 2 days
Buoyance or fall velocity of eggs and/or young larvae	Neutrally buoyant and distributed in water column
Vertical migration	None. Distributed throughout water column or to 10 m
Larval 'sensing' capacity	Yes, to 1km during competency phase
Maximum larval duration (days)	12 days (+/- 30% to 8 and 16 days)
Spawning seasonality	Annually, October to February
Number of source/destination IDs	95 reef patches, each acting as potential source and destination
Precision of connectivity estimates	1/100,000,000 larvae
Release frequency	Fortnightly
Total number of larval releases per reef per spawning season	10
Wall-time for individual simulations and complete ensembles	~7 hrs per simulation 124 days (wall-time) to complete two ensembles

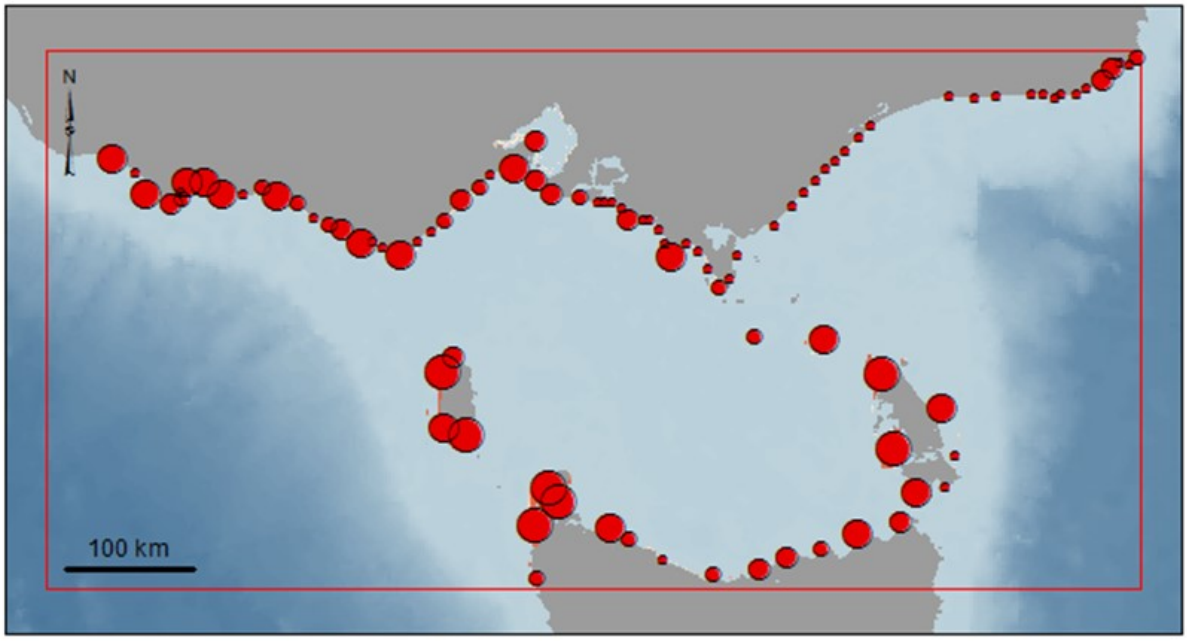

Figure A3: Abalone connectivity model domain. The model includes all rocky reef habitat of Victoria and Bass Strait, at a resolution of 1 km. All unique habitat patches (95 in total) are represented by red nodes, where the size of each node is shown relative to the area it represents.

The seascape model for abalone was developed based on the best-available reef habitat data derived from substrate classifications of the merged LiDAR and multibeam datasets. To reduce the number of individual reefs, the substrate raster was resampled to 500 m and converted to polygons representing rocky reef locations at a 500 m resolution. These habitat data were rescaled and projected onto our modelled seascape (Figure A3). Hydrodynamic data quantifying the nearshore and far-field ocean currents around Victoria and the regional seascape were obtained from DHI-MIKE data from Water Technology for local-scale depth-averaged and high spatial-temporal resolution products. The MIKE data were provided by Water Technology at 5-minute time-steps for all years between 1990 and 2015 at a horizontal resolution ranging between 500-800 m within ~7km of the shoreline, to ~10 km resolution through Bass Strait, and up to 25-35 km in the open ocean. We modelled abalone dispersal across 1-hourly currents at 1 km resolution derived from Water Technology coastal model. The abalone dispersal simulations were modelled for up to a 20-day larval duration period

(potential settlement from 2.5 days) to explore the impact of uncertainty in the maximum larval duration parameter.

To develop maps showing the spatial structure of potential population connectivity via larval dispersal, we summarised the three model ensembles as a probability matrix to show the likelihood of movement through the seascape and as a migration matrix to show the relative influence on downstream populations. We used network algorithms to uncover the emergent structure within these networks, revealing natural clusters of tightly linked populations. Boundaries between these network 'communities' show regions where larval flow may be lower indicating sub-population boundaries.

To identify those reefs or populations that may serve as strong and persistent larval sources, we used four complementary measures of replenishment: i) Outflow quantifies each source's contribution to other sites, ii) Local retention is the proportion of larvae released from each source that settles in that focal patch (derived from the probability matrix), iii) Inflow measures the total relative amount of larvae settling to each patch (including those larvae that are locally produced), and iv) the sourceness metric quantifies the relative source-strength of each patch as Outflow/Inflow (Cronin 2007, Pulliam 1988).

Stepping-stone habitat patches or populations are those sites that may fall along dispersal pathways connecting a high proportion of sites within the seascape. Important stepping-stone sites were identified using the betweenness centrality measure from graph theory. Here, we transformed the migration matrix to be the same rank-order as geographic distance ($\log[M]^{-1}$) and used the betweenness centrality to quantify the relative strength of centrality of each population. Those sites with a high value reflect populations which are consistently important in maintaining flow among a large proportion of sites. Mapping these sites with respect to the

community structure (above) and dispersal networks reveals the geographic structure of stepping-stones.

The spatial structure of biomass, abundance, and genetic variation may be driven, in part, by the dispersal dynamics of the species of interest. The dispersal structure, as well as the environmental setting, local demographics and population history, may play a significant role in persistence, health, and sustainable fishing level of individual populations. To aid in the analysis of the biomass and genetic data, we provided several additional dispersal-based metrics capturing connectivity patterns: i) self-recruitment quantifies the relative proportion of settlers at each destination site that originated from that focal site (diagonal of the migration matrix), ii) in-degree is the total number of 'significant' connections coming into a destination site (ignoring the strength of individual connections) derived from the migration matrix, and iii) out-degree which is the total number of 'significant' dispersal connections originating from a source site that leads to destination patches. For in- and out-degree, a significant connection was counted if it contributed to more than 0.1% of settlers to a destination site in the migration matrix.

Comparison of Biomass from Models and Fishery Estimates

Using the predictive maps of abalone density (kg/900m^2) we calculated the total biomass within each of the three Victorian abalone fishery zones for each year: Eastern, Central, and Western. Using the total allowable catch (TAC) set by the Victorian Fisheries Authority, we also calculated the total exploitable biomass (TEB) from each region during years when TAC was available (Eastern: 1998 – 2015, Central: 2006 – 2015, and Western: 2006 – 2015). To calculate TEB, we used the following equation:

$$TEB = TAC \times 6.6$$

To determine how well the model predictions match up with the TEB, we ran a regression to compare the two sets of predictions.

Results

Table A4: Results from the Emerging Hot Spot Analysis completed on summer sea surface temperature (SST). Each of the patterns detected during the analysis is shown along with the percentage of that pattern from each Victorian abalone fishing zone. The final column shows the percentage of each pattern across the entire state.

EMERGING HOT SPOT RESULTS – SUMMER SEA SURFACE TEMPERATURE

	Percentage of Region within Pattern			
Emerging Hot Spot Analysis Pattern	**Victorian Western Abalone Zone**	**Victorian Central Abalone Zone**	**Victorian Eastern Abalone Zone**	**All Victoria**
No Pattern Detected	70.3%	34.9%	61.6%	44.1%
New Hot Spot	0.0%	0.3%	13.7%	2.2%
Intensifying Hot Spot	0.0%	17.7%	0.0%	12.5%
Consecutive Hot Spot	0.0%	13.7%	0.0%	9.7%
Oscillating Hot Spot	0.0%	9.4%	24.7%	10.3%
Sporadic Hot Spot	0.0%	12.0%	0.0%	8.5%
Diminishing Cold Spot	24.3%	12.0%	0.0%	12.1%
Persistent Cold Spot	5.4%	0.0%	0.0%	0.8%

Table A5: Results from the Emerging Hot Spot Analysis completed on annual max current speed. Each of the patterns detected during the analysis is shown along with the percentage of that pattern from each Victorian abalone fishing zone. The final column shows the percentage of each pattern across the entire state.

EMERGING HOT SPOT RESULTS – ANNUAL MAX CURRENT SPEED

	Percentage of Region within Pattern			
Emerging Hot Spot Analysis Pattern	**Victorian Western Abalone Zone**	**Victorian Central Abalone Zone**	**Victorian Eastern Abalone Zone**	**All Victoria**
No Pattern Detected	5.8%	37.2%	28.9%	31.6%
Intensifying Hot Spot	0.0%	12.9%	68.7%	18.7%
Persistent Hot Spot	0.0%	9.0%	1.2%	6.6%
Consecutive Hot Spot	0.0%	5.5%	0.0%	4.0%
Historical Hot Spot	0.0%	0.0%	1.2%	0.2%
Sporadic Cold Spot	1.2%	1.8%	0.0%	1.5%
Persistent Cold Spot	0.0%	0.5%	0.0%	0.3%
Consecutive Cold Spot	26.7%	6.4%	0.0%	8.4%
Intensifying Cold Spot	65.1%	23.0%	0.0%	25.8%

New Cold Spot	1.2%	3.7%	0.0%	2.8%

Table A6: Results from the Emerging Hot Spot Analysis completed on winter max wave orbital velocities. Each of the patterns detected during the analysis is shown along with the percentage of that pattern from each Victorian abalone fishing zone. The final column shows the percentage of each pattern across the entire state.

EMERGING HOT SPOT RESULTS - WINTER MAX WAVE ORBITAL VELOCITIES

	Percentage of Region within Pattern			
Emerging Hot Spot Analysis Pattern	**Victorian Western Abalone Zone**	**Victorian Central Abalone Zone**	**Victorian Eastern Abalone Zone**	**All Victoria**
No Pattern Detected	17.4%	38.6%	65.1%	39.2%
New Hot Spot	1.2%	0.2%	0.0%	0.3%
Intensifying Hot Spot	66.3%	16.1%	8.4%	22.1%
Persistent Hot Spot	9.3%	0.2%	0.0%	1.5%
Consecutive Hot Spot	5.8%	0.5%	2.4%	0.7%
Sporadic Hot Spot	0.0%	5.3%	6.0%	5.5%
Sporadic Cold Spot	0.0%	4.4%	8.4%	4.3%
Consecutive Cold Spot	0.0%	1.1%	1.2%	1.0%
Persistent Cold Spot	0.0%	27.1%	8.4%	20.7%
Intensifying Cold Spot	0.0%	6.4%	0.0%	4.8%

Biophysical Modelling

The DHI-driven dispersal model for abalone resulted in an average dispersal network (averaged across 217 simulations over 25 years) revealing general west-to-east connectivity of larvae (Figure A4). Some connectivity appears to exist between the reefs of Tasmania and into eastern Victoria across Bass Strait. Strong larval sources which are key to regional replenishment were identified primarily using the Outflow metric quantifying the total relative contribution each population provides to downstream habitat patches. Identifying and mapping these key populations clearly shows the distribution of source patches (Figure 15). The primary sources of abalone larvae are from those large populations in the west half of the state, with a few strong sources in the east and along northern Tasmania. Strong source populations for SRL are more continuously distributed across the seascape without strong clustering (Figure 15, bottom).

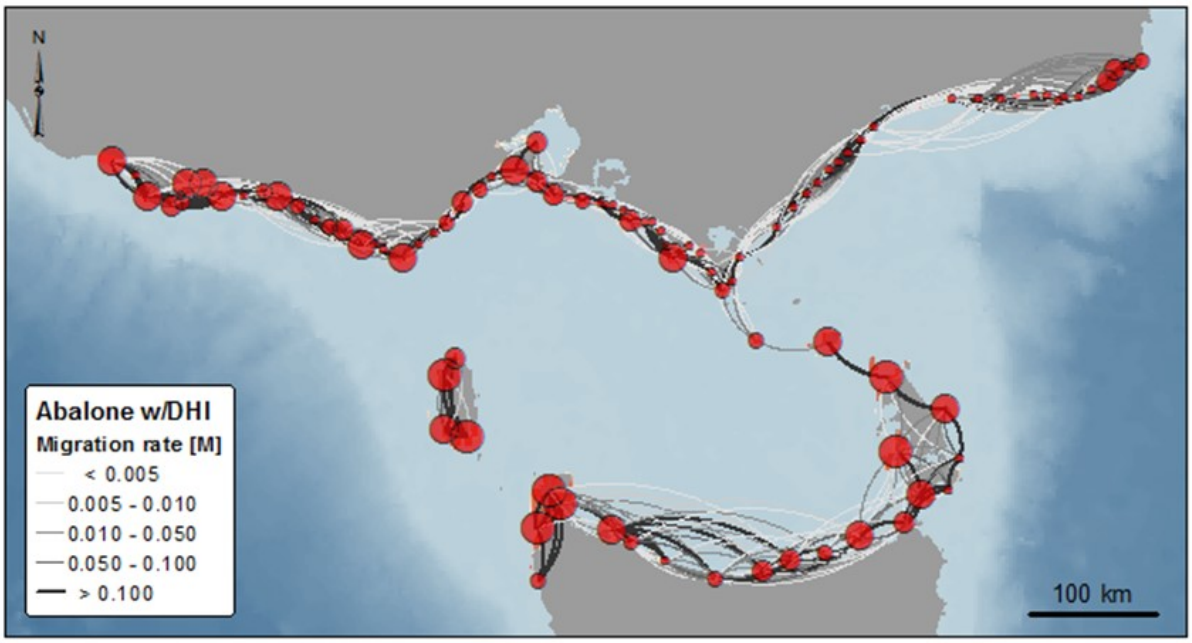

Figure A4: Abalone dispersal network from DHI local-scale ocean currents. The dispersal network for abalone derived from the migration matrix where the strength and direction of connectivity are illustrated by the weight and bend of the links (direction following clockwise).

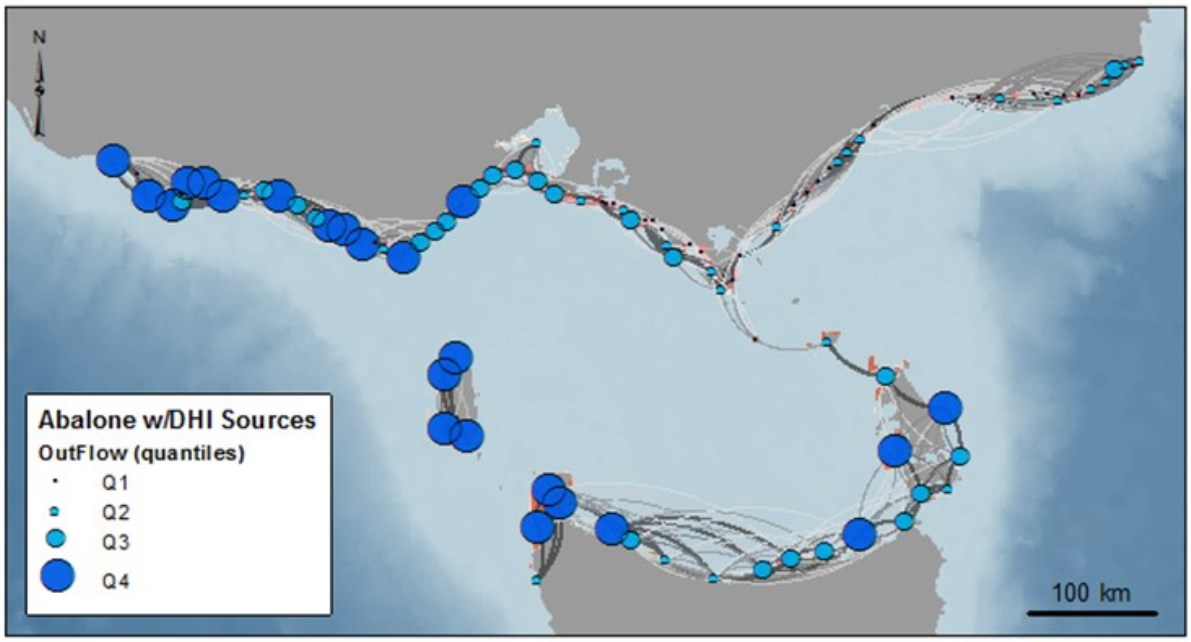

Figure A5: Strong larval sources. Sourceness based on the OutFlow metric for abalone with DHI currents. The strongest average sources are those shown in dark blue (top quantile) for each ensemble. Size of the nodes represent the strength of replenishment to neighbouring populations.

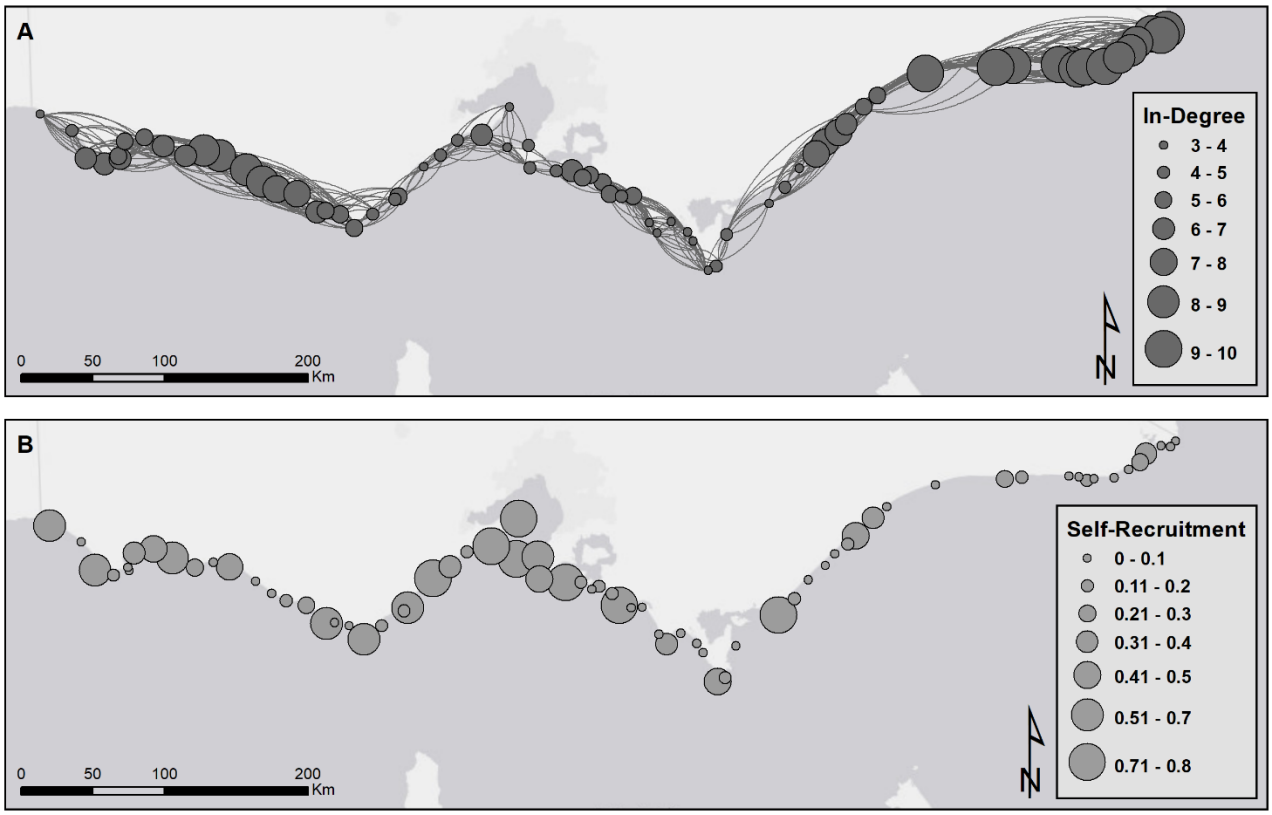

Figure A6: *Haliotis rubra* connectivity patterns across Victoria, Australia. In-degree (A) shows total number of significant connections coming into a designated site. Each circle represents a separate reef in the network and the gradation in circle size corresponds to increasing numbers of sources supplying that reef. The lines represent the significant connections between reefs. Self-recruitment (B) quantifies the relative proportion of settlers at each destination site that originated from that focal site. Again, the circles represent individual reefs and the size of circle increases as self-recruitment increases. Service Layer Credits for the basemap image: Esri, HERE, DeLorme, MapmyIndia, © OpenStreetMap contributors, and the GIS user community.

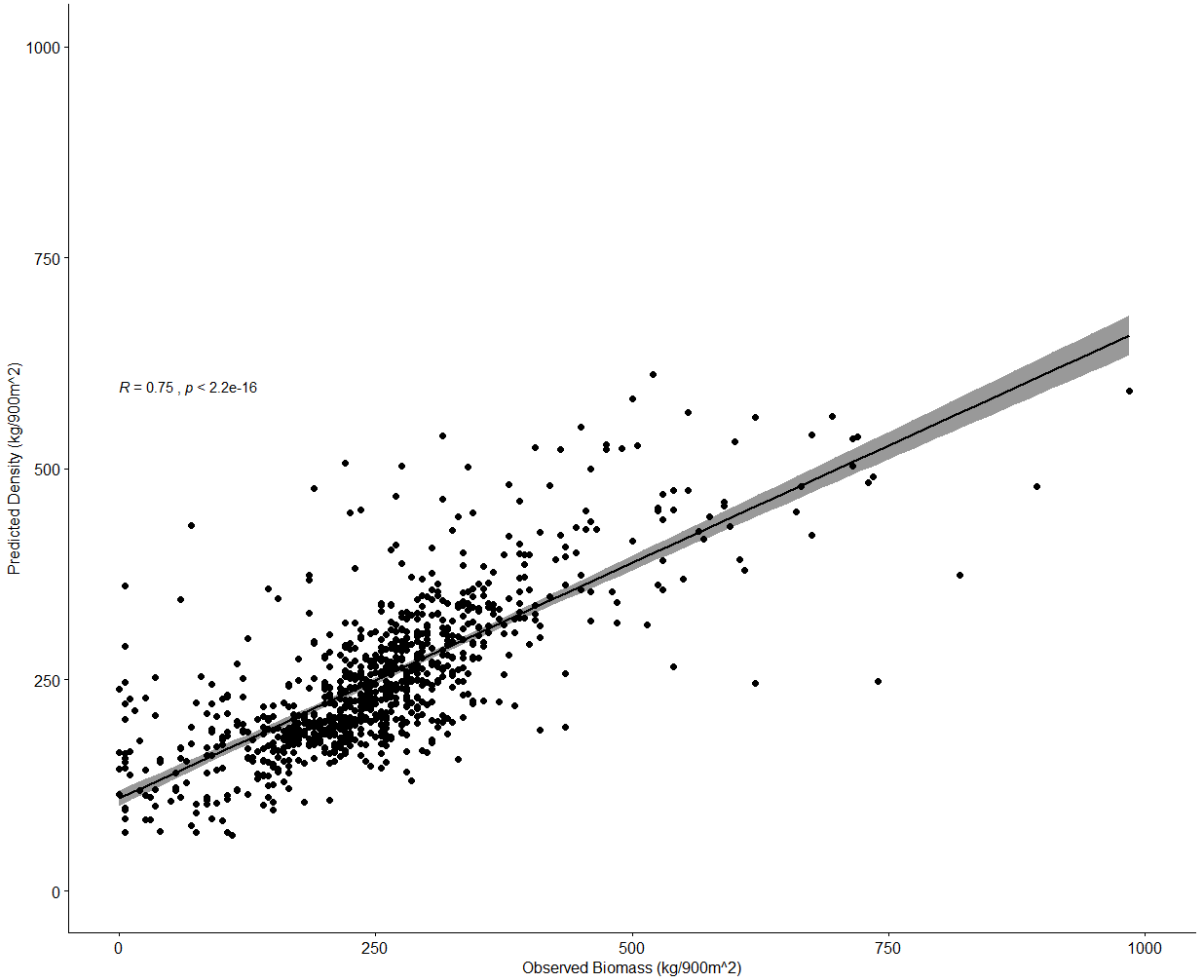

Figure A7: Comparison between observed *Haliotis rubra* density and density predicted from the boosted regression tree (BRT) model in the evaluation dataset, which was reserved for testing the prediction accuracy of the BRT model. The Pearson correlation (*R*) is shown on the figure with its associated *P*-value.

Comparison of Biomass from Models and Fishery Estimates

The comparison between the total biomass estimates from each fishery zone and the corresponding TEB for those fishery zones show that there is fairly good agreement across estimates with a statistically significant R^2 value of 0.72 (*P*-Value < 0.001; Figure A8).

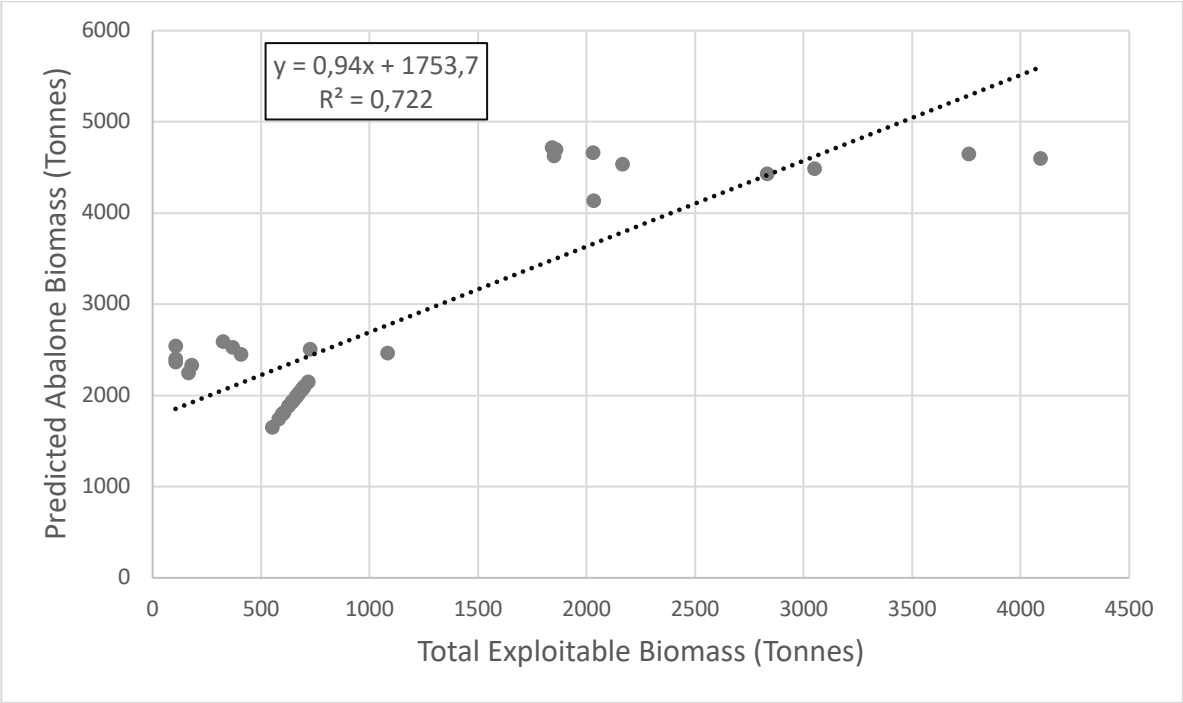

Figure A8. Comparison between the predicted abalone biomass from the boosted regression tree (BRT) models and the total exploitable biomass calculated from the fishery zone total allowable catch. The equation for the regression line and the R^2 are also shown.

References

Cronin, J. T. 2007. From population sources to sieves: the matrix alters host-parasitoid source-sink structure. - Ecology 88: 2966-2976.

ESRI 2011. ArcGIS Desktop: Release 10. - In: Environmental Systems Research Institute.

Pulliam, H. R. 1988. Sources, sinks, and population regulation. - The American Naturalist 132: 652-661.

Treml, E. A., et al. 2012. Reproductive output and duration of the pelagic larval stage determine seascape-wide connectivity of marine populations. - Integrative and Comparative Biology 52: 525-537.

Treml, E. A., et al. 2015. Identifying the key biophysical drivers, connectivity outcomes, and metapopulation consequences of larval dispersal in the sea. - Movement Ecology 3: 1-16.